Microholography of Living Organisms

Johndale C. Solem and George C. Baldwin

Summary. By using intense pulsed coherent x-ray sources that are currently under development, it will be possible to obtain magnified three-dimensional images of elementary biological structures in the living state at precisely defined instants. For optimum contrast, sensitivity, and resolution, the hologram should be made with x-rays tuned to a resonance of nitrogen near 0.3 nanometer. Resolution will then be limited mainly by the hydrodynamic expansion that occurs while the necessary number of photons is being registered. Problems of technique are also briefly discussed.

Efforts are being made in many laboratories throughout the world to develop new sources of coherent x-radiation. A major incentive for these efforts is the possibility of making diffraction-limited holograms of microscopic structures, with correspondingly high resolution (*1*). There is hope that laser-like sources, emitting subnanosecond bursts of intense monochromatic x-radiation, will soon be available for wavelengths between 0.1 and 10 nanometers; hence it is timely to consider the problems that their holographic applications may involve, the advantages that snapshot x-ray holography may have over other techniques, and the constraints that those applications will impose on system design and performance.

We believe that a particularly promising application of snapshot x-ray holography will be to the study of microscopic biological structures in the living state (*2*). X-rays offer not only high resolution, but also very high contrast ratios (*2*) for the important structures within living organisms. Staining of specimens, frequently essential for optical and electron microscopy, is unnecessary in x-ray holography when the wavelength is properly chosen. Subnanosecond resolution, which would eliminate blurring by thermal motion and by normal biological activity, is promised by several new types of x-ray sources under development. X-ray exposure kills the organism, just as fixing or staining does, but with short-pulse holography the normal biological integrity can be preserved until the actual moment of exposure, permitting the living state at that moment to be revealed with complete three-dimensional information (*3*).

In this article, we briefly summarize the findings of a comprehensive study of the problems peculiar to biomicroholography (*4*). Symbols used throughout the article are defined in (*5*).

Sources for X-ray Holography

To be suitable for holography, x-radiation must be monochromatic with a relatively high degree of coherence—the property that enables two waves to interfere, constructively or destructively (*6*). Coherence can be (loosely) characterized by an effective finite length of photon wave trains. Two overlapping wave trains produce interference fringes or simply an incoherent background, depending on the extent to which they overlap and on the constancy of their respective phases.

Electrons bombarding heavy-element targets in conventional x-ray tubes and plasmas generate bremsstrahlung, which is not monochromatic, and characteristic line radiation, which, although quasi-monochromatic, has insufficient coherence for diffraction-limited holography and is available at only a small number of discrete wavelengths. On the other hand, there are new sources under development that are characterized by high intensity and monochromaticity, some with tunability and coherence. Recent conferences (*7*) have devoted entire sessions to the development and application of sources of shortwave coherent radiation.

Nonlinear optical frequency multiplication techniques have been demonstrated (*8*) with which ultraviolet radiation from lasers is upconverted to wavelengths as short as 40 nm, and they promise to reach still shorter wavelengths, generating intense picosecond pulses of tunable coherent radiation.

By using magnetic undulators (*9*), quasi-monochromatic synchrotron radiation can be generated with high intensity. Fusion laser systems can create dense plasmas in which suprathermal electrons (*10*) generate intense x-radiation. Although these sources are intense, however, neither may meet coherence requirements.

X-ray (*11*) and gamma-ray (*12*) lasers are under development, and stimulated emission gain has been reported for several x-ray transitions (*13*). X-ray lasers will be inherently short-pulse, high-intensity devices. This is because (i) they will probably not have resonant cavities, so the radiation being amplified can make only a single passage through the active medium and (ii) the creation and maintenance of a high density of excited atomic states of short lifetime and high quantum energy requires enormous power (*11*), which can be supplied only on a pulsed basis.

Geometries for X-ray Holography

In holography, wave interference is used to register information about both the amplitude and the phase of a monochromatic wave at a reference surface (*14*). Once recorded, this information can be used to infer the geometric configurations of the objects that, by scattering or absorption, contributed to the structure of the registered wave. Such "wave front reconstruction" is accomplished either by coherent illumination of the hologram or by an equivalent computer analysis. Reconstruction gives rise to real and virtual images (*15*) of the objects, displayed in three dimensions, with magnifications determined by the ratio of the wavelengths of the original and reconstructing illuminations and with a resolution that, given an appropriate recording medium and holographic technique, is limited only by diffraction (*16*).

Registration of the hologram requires that the reference radiation be coherent

Johndale C. Solem is assistant division leader in the Theoretical Division and George C. Baldwin is a staff member in the Physics Division, Los Alamos National Laboratory, Los Alamos, New Mexico 87545.

0036-8075/82/1015-0229$01.00/0

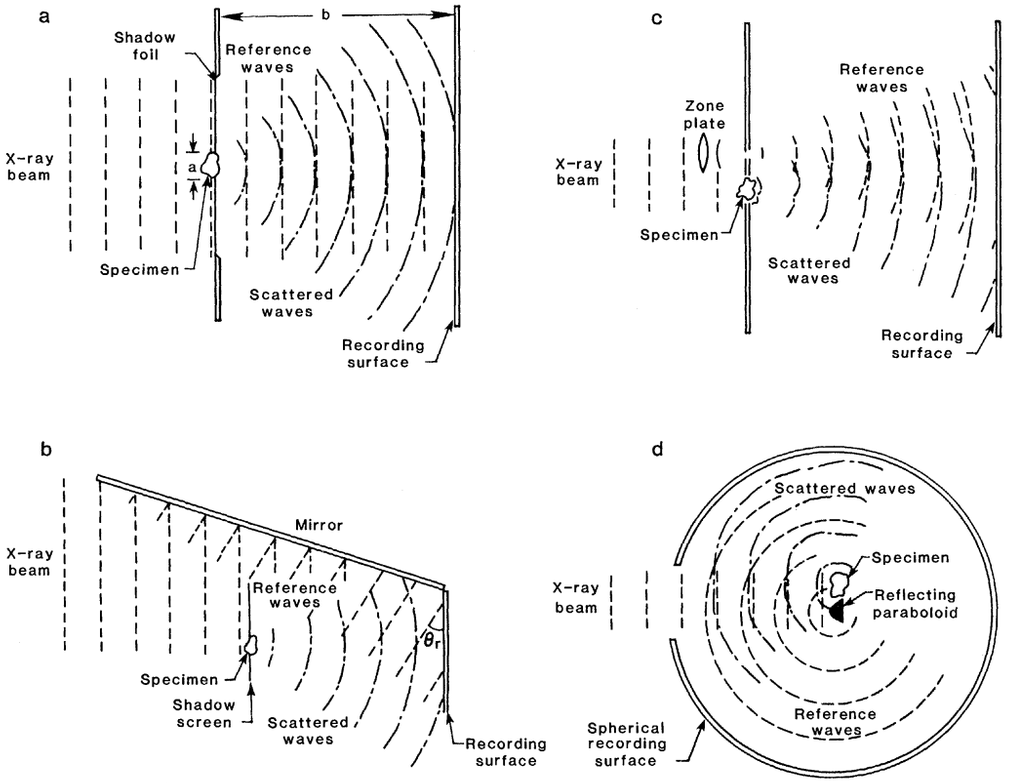

Fig. 1. Four basic geometries for holography. In (a) and (b) the reference waves are plane; in (c) and (d) they are spherical.

Table 1. Comparison of holographic techniques.

Characteristic	Fresnel transform Fig. 1a	Leith-Upatnieks Fig. 1b	Fourier transform Fig. 1c	Fourier transform Fig. 1d
Geometry				
Reference wave front	Plane	Plane	Spherical	Spherical
Reference surface	Plane	Plane	Plane	Spherical
Reference source	Distant, in-line	Distant, off-axis	Point or equivalent (zone plate or parabolic reflector)	
Advantage	Simplicity	Separation of real and virtual images	Less sensitivity to grain size	(i) 4π recording; (ii) less sensitive to recording surface roughness
Difficulties	Resolution limited by grain size		Survivable high precision zone plate	Well-characterized reflector
Registration	Temporal coherence requirements	Mirror requirements	Trade-off between ϵ and Δ^2	
Reconstruction	Obscuration by virtual image unless $b\lambda \gg d^2$	$\theta_r > \sin^{-1}(\lambda/\delta)$	Dynamic reference wave front distortion	
Coherence requirements				
Spatial	$2\frac{b\lambda}{\delta\mu}$	$3\frac{b\lambda}{\delta\mu}$	$2a$	
Temporal	$\frac{b}{1-\xi}(\mu^{-1}-1)$	$\frac{2}{\pi}\frac{b}{1-\xi}(\mu^{-1}-1)$	$\mu\frac{a^2}{2b(1-\xi)}$	$\frac{a^2}{2b(1-\xi)}$
Maximum specimen volume				
Coherence limit	$\pi\frac{\delta\lambda^2(1-\xi)^2x^2}{\Delta^2(\mu-1)^2}$	$\frac{\pi^3}{4}\frac{\delta\lambda^2(1-\xi)^2x^3}{\Delta^2(\mu-1)}$	$\mu^{-3/2}\frac{\pi}{6}[2xb(1-\xi)]^{3/2}$	$\frac{\pi}{6}[2xb(1-\xi)]^{3/2}$
Mapping limit			$(\mu^{-2}-1)\frac{\pi b^2\delta^3}{\Delta^2}$	$2(1-\mu)\frac{\pi b^2\delta^3}{\Delta^2}$
Reference	(*14*)	(*20*)	(*21*)	(*39*)

with the radiation that has interacted with the object being holographed and, if diffraction-limited resolution is to be approached, that the grains of the recording medium be smaller than the closest spacings of interference fringes on its surface. Incoherent radiation and statistical fluctuations of response in the recording medium give rise to background (noise).

Essential features of the principal geometries for holography are shown in Fig. 1 and compared in Table 1. In all types, the spacing of interference fringes in the hologram is determined by the wavelength, the dimensions of structural detail in the object, and the geometry of the interfering waves (that is, plane or spherical) (*17*).

Plane-wave reference is inherently simple, but is sensitive to grain size in the recording medium (*18*) and to overlap of the real and virtual images (*19*). The Leith-Upatnieks modification (*20*) of the in-line geometry reduces the image-overlap problem, but at the expense of requiring a mirror and a broadened beam for system illumination; both may be difficult at x-ray wavelengths. The Fourier transform geometries, having curved wave fronts, achieve large fringe spacings and are therefore less sensitive to grain size (*21*). Although sometimes (*16*) called lensless, they are not really so; a Fresnel zone plate (*22*) or paraboloidal reflector (*23*) is needed to create the point source of reference radiation (*3*). Owing to diffraction, the equivalent source is not a true point. With the zone plate, this limits the resolution to twice the spacing of the outermost zone (*3*).

Both coherence length and geometry limit the holographable volume of a specimen. The term mapping limit in Table 1 refers to the fact that a hologram is a homomorphic mapping of specimen volume onto the surface of the recording medium. The terms "Fresnel" and "Fourier" characterize the nature of the mapping transformation.

Interactions of X-Radiation

Formation and registration of the interference fringes on a hologram that reveal the presence of an object is made possible by the elementary interactions of absorption and scattering in the specimen and the recording medium. In the x-ray region, elementary interactions of radiation not only excite quantized states in molecules, but also ionize and break chemical bonds. The interactions include both nonresonant and resonant processes—that is, both slowly and rapidly varying functions of wavelength. Scattering may be either elastic (coherent) or inelastic (incoherent or Compton). As noted above, incoherent scattering contributes to noise in the hologram.

Figure 2 shows cross sections (*24*) for absorption and scattering by light elements that are abundant in biological matter, as functions of wavelength in the range where absorption is mainly by the photoelectric effect. The photon energy

$$E = (hc/e)\lambda^{-1} = 1234.8/(\lambda, \text{nm}) \text{ eV} \quad (1)$$

is expended in ejecting a bound electron and creating, in the subsequent atomic relaxation, an Auger electron cascade and secondary photons. Discontinuities in the photoelectric cross section therefore exist at the binding energies of the *K*-shell, the *L*-shell, and so on (*25*).

Near the absorption edge of nitrogen (409.9 eV), a narrow resonance is observed at a photon energy sufficient to excite a *K* electron into a weakly bound higher quantum state but insufficient for ionization. In the atomic case, the transition is $1s^2 2s^2 2p^3 \rightarrow 1s^1 2s^2 2p^3 3p^1$. In nitrogen compounds there are similar resonances, in which a core electron is excited into the lowest unfilled molecular orbital; for example, in N_2 there is a resonance at a photon energy of 401.3 eV (*26*). In N_2O, with two nitrogen atoms in different environments, resonances occur at 401.2 and at 404.9 eV (*27*). For both molecules, the maximum cross section (*27*) is about 1.7×10^{-17} square centimeters. It is probable that research in progress will reveal similar strong resonances in organically bound nitro-

Table 2. X-ray absorption lengths for most abundant biological constituents.

Constituent	X-ray attenuation length (nm)				
	200 eV	400 eV	800 eV	1600 eV	Nitrogen *K*-shell resonance
Water	8.45×10^2	4.69×10^3	1.34×10^3	8.72×10^3	4.69×10^3
Protein	9.31×10^2	6.75×10^2	1.96×10^3	1.34×10^4	6.93×10^1
DNA	6.31×10^2	7.83×10^2	1.82×10^3	1.22×10^4	7.20×10^1
RNA	6.31×10^2	8.23×10^2	1.77×10^3	1.18×10^4	7.58×10^1
Lipid	1.58×10^3	5.34×10^2	2.28×10^3	1.57×10^4	5.34×10^2
Carbohydrate	1.08×10^3	8.51×10^2	1.64×10^3	1.09×10^4	8.51×10^2

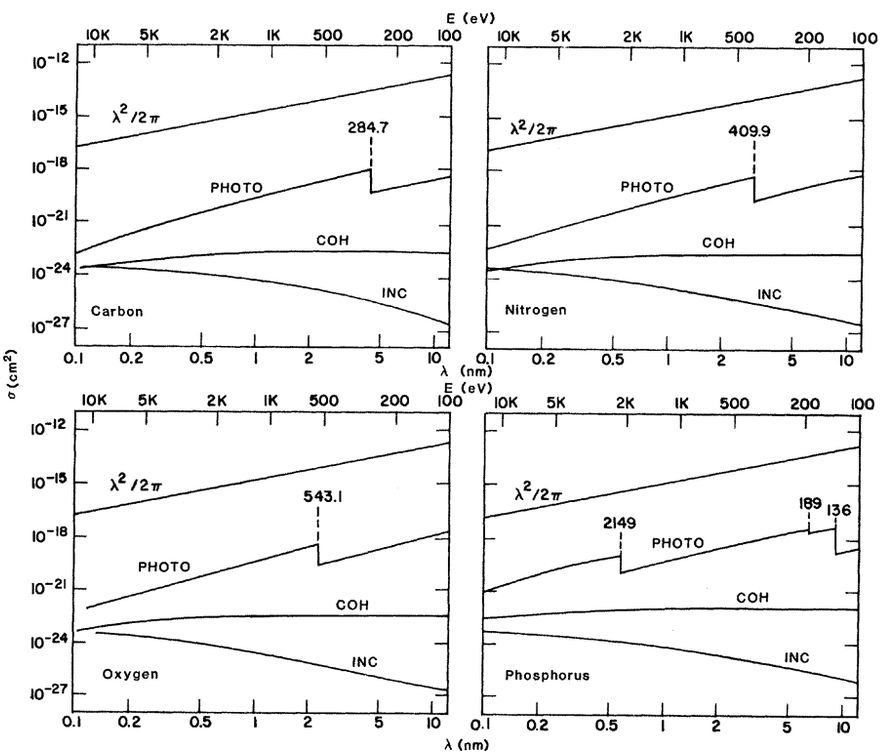

Fig. 2. Cross sections for interaction of photons with atoms of four biologically important elements, in the wavelength region 0.1 to 10 nm. Key: *PHOTO*, photoelectric absorption; *COH*, coherent or elastic scattering; *INC*, incoherent or inelastic scattering; $\lambda^2/2\pi$, the maximum possible cross section for a resonant interaction.

gen, such as that in proteins and nucleic acids (*28*).

Attenuation lengths [distances for which intensity is reduced by the factor exp(−1)] of important biochemical constituents are listed in Table 2 for several photon energies. Note that, at the energy of the nitrogen resonance, water and carbohydrates are relatively transparent in comparison with proteins, DNA, and RNA. This has great significance for biomicroholography, as it enables important constituents to be revealed with high contrast by using x-radiation of wavelength 3 nm (*2*, section 2.1) and with maximum contrast when tuned to the nitrogen resonance. In Fresnel transform holography, the high contrast ratio reduces the coherence length necessary to avoid obscuration by the virtual image in reconstruction (see Table 1), because the required coherence length depends on the size of the largest opaque structure in the specimen, rather than the total specimen size (*19*).

The interactions described above do not occur independently in condensed matter. In proteins, the density of nitrogen atoms is so high that the spacing of neighboring atoms is comparable with the resonance wavelength and the atoms do not all see the same intensity. Interference and attenuation then combine to determine an effective cross section for a protein molecule. In the following, we assume that protein molecules are roughly spherical in outline (*29*); the effective absorption cross section is taken to be the product of geometric area by the attenuation factor; and the effective scattering cross section the product of geometric area by the square of that factor (*4, 30*).

To be a good candidate for x-ray holographic investigation, a specimen not only must display a large contrast ratio between the features we are seeking to image, but also must be reasonably transparent to the x-rays. Table 3 lists examples of biological specimens that might be candidates for x-ray holography. The specimens range over 13 orders of magnitude in total mass, and it appears that the largest specimen for which we could expect sufficient transmission has a mass of about 10^{-8} gram. Larger specimens, which are generally not symmetrical, might be aligned to reduce the total distance that the x-rays must travel through the specimen. By pressing the specimen between the front and rear windows of the specimen holder, living cells as massive as 10^{-7} g might be holographed.

Factors Affecting Resolution

Requirements of snapshot biomicroholography. If the 3-nm wavelength that ensures optimum contrast is to give spatial resolution adequate for microbiological investigations, with an appropriate holographic geometry and a recording medium sensitive to this wavelength, it must be possible to register a sufficient number of photons that have been elastically scattered from each resolution element of the specimen (in excess of those inelastically scattered) before the specimen has been essentially altered, killed, or destroyed by the radiation.

Existing x-ray sources, in particular synchrotron radiation sources, have been used to make holograms (*31*), but they require long exposures, which limit their usefulness for research on living specimens. Other, more coherent sources may also be developed, but those of low intensity will be similarly limited, since ionization will have decomposed molecules, modified compositions, and destroyed organisms long before enough radiation can be received to form a useful hologram. Snapshots would seem to be essential for microholography of living systems. Fortunately, it is likely that brief, intense bursts will

Table 3. Mass, dimensions, and x-ray transmission of various biological specimens.

Specimen	Mass (g)	Greatest dimension (nm)	Characteristic dimension (nm)	X-ray transmission (homogenized)				
				200 eV	400 eV	800 eV	1600 eV	Nitrogen *K*-shell resonance
Tobacco necrosis viron	10^{-18}	20	10	0.987	0.986	0.995	0.999	0.868
Escherichia coli phage $\phi \times 174$	10^{-17}	20	20	0.977	0.972	0.990	0.998	0.754
Mycoplasma laidlawii	10^{-16}	~ 50	~ 50	0.944	0.984	0.968	0.995	0.984
Vaccinia viron	10^{-15}	200	100	0.901	0.859	0.950	0.992	0.208
Mycoplasma gallisepticum	10^{-14}	250	250	0.750	0.923	0.850	0.976	0.921
Immature *E. coli* bacterium	10^{-13}	1,000	450	0.596	0.879	0.745	0.957	0.873
Mature *E. coli* bacterium	10^{-12}	2,000	1,000	0.317	0.751	0.520	0.906	0.739
Anthrax bacterium	10^{-11}	3,000	2,000	0.101	0.564	0.270	0.821	0.546
Red blood cell (human)	10^{-10}	8,000	4,500	0.005	0.315	0.046	0.627	0.303
Monas (small protozoan)	10^{-9}	10,000	10,000	9.19×10^{-6}	7.65×10^{-2}	1.09×10^{-3}	3.55×10^{-1}	7.04×10^{-2}
Amoeba (dysentery)	10^{-8}	20,000	20,000	8.45×10^{-11}	5.84×10^{-3}	1.18×10^{-6}	1.26×10^{-1}	4.96×10^{-3}
Smooth muscle cell	10^{-7}	500,000	45,000	2.17×10^{-23}	9.48×10^{-6}	4.63×10^{-14}	9.46×10^{-3}	6.54×10^{-6}
Paramecium (large protozoan)	10^{-6}	300,000	100,000	4.32×10^{-52}	6.87×10^{-12}	2.33×10^{-30}	3.18×10^{-5}	3.01×10^{-12}
Ovum (human)	10^{-5}	200,000	200,000	$< 10^{-100}$	4.72×10^{-23}	5.42×10^{-60}	1.01×10^{-9}	9.04×10^{-24}

be typical of near-term coherent x-ray source developments.

Hydrodynamic blurring. With an intense pulsed coherent source (such as an x-ray laser) it will be hydrodynamic expansion, initiated by sudden heating, rather than normal biological activity, chemical change, or thermal agitation, that limits the time during which recording of the hologram must be accomplished (*3*).

Analytical expressions for the explosion of a protein globule are useful for estimating the radiation requirements for typical cases (*4*). Although approximate, they compare well with exact numerical calculations. They are based on the criterion that, to achieve a linear resolution δ, a specified minimum number of photons must have been coherently scattered in a volume δ^3 and that, during the exposure time Δt, no dimension of the specimen should have increased by more than δ.

Maximum exposure time. To examine the structure of protein units within a cell with resolution $\delta < d$, the maximum exposure time is found to be

$$\Delta t = \delta^{2/3}/(FIK\Sigma_a)^{-1/3} \qquad (2)$$

where the dimensionless coefficient F is a function of the equation-of-state parameters of the materials involved and the rate at which transport processes remove energy from the exploding protein. Longer exposures result in blurring; that is, the resolution achieved will correspond to a larger value of δ.

If, on the other hand, linear resolution larger than the characteristic dimension of the protein globule is acceptable, then the exposure time found above should be multiplied by the factor δ/d, after substituting a different dimensionless coefficient G (*4*).

If the laser burst duration exceeds the value found above, then some shutter mechanism must be provided for the incident radiation, or a time gate must be provided for recording. Several possibilities will be discussed in a later section.

Intensity requirement. The number of photons elastically scattered from a single resolution element and registered in the hologram during the maximum exposure time is approximately

$$N = \epsilon K \rho I \Sigma_e \delta^3 \Delta t / Ee \qquad (3)$$

and it must exceed the incoherent photon background by a statistically significant number (the signal-to-noise ratio).

By combining Eqs. 2 and 3, we obtain the formula (*4*)

$$I \approx \frac{1}{K}\left(\frac{N\,eE}{\Sigma_e\,\rho\,\epsilon}\right)^3 \frac{\Sigma_a}{\delta^{11}} \times \begin{cases} \sqrt{F}, & \delta < 3d/8 \qquad (4a) \\ \sqrt{G(d/\delta)^3}, & \delta > 3d/8 \qquad (4b) \end{cases}$$

which states, in terms of measurable parameters, the laser intensity required to obtain a specified resolution in an exposure for the maximum time before unacceptable hydrodynamic blurring can occur.

Note the extremely strong (5.5- and 7-power) dependences on the linear resolution δ. Should we wish to improve resolution by a factor of 2, we must increase laser intensity by two orders of magnitude, because the statistically significant number N of useful photons would then have to be scattered in a shorter time by a smaller volume element.

Recording the Hologram

For well-defined interference fringes in the hologram, the reference wave and the scattered waves must have comparable amplitudes and coherence lengths appropriate to the geometry (Table 1). The number N in Eqs. 3 and 4 involves the recording medium as well as properties of the specimen, the radiation, and the geometry. An x-ray hologram can be registered by photoelectron emission and by either prompt or latent chemical change induced by the radiation.

Photographic emulsions are commonly used for optical holography and even for x-ray holography (*31*), but, even at long wavelengths, grain size is troublesome. One would prefer a "grainless" medium, that is, one with linear resolution limited only by its atomic or molecular structure.

Electron emission has been proposed for x-ray holography (*32, 33*). If an electron microscope could be used to image the points of electron emission from a photocathode reference surface, time-gated holography (*33*) might be possible. However, the continuous distributions in energy and in angles of emission of electrons preclude the formation of sharp electron-optical images; this imposes a trade-off between quantum efficiency and resolution (*3*) unless image-deblurring analysis can be applied.

Photoresists (materials that lose resistance to chemical etching at points exposed to radiation) have resolutions that can approach 10 nm (*34*). In polymethylmethacrylate (PMMA), for example, polymeric chains are broken by ionizing radiation. Its resolution is best for 3-nm

Table 4. High-intensity holography.

Characteristic	100-nm protein structures in transparent cytoplasm	Globular protein molecules in lipid bilayer membrane
Feature dimension (d), cm	10^{-5}	2.5×10^{-7}
Required resolution (δ), cm	10^{-6}	10^{-6}
Required photon statistics (N/ϵ)	10^3	10^3
Elastic cross section of feature (Σ_e), cm^2	3.0×10^{-11}	4.1×10^{-16}
Absorption cross section of feature (Σ_a), cm^2	4.9×10^{-11}	9.0×10^{-15}
Equation of state and heat transport constant	$F = 0.035$	$G = 0.086$
Features per gram (K), g^{-1}	1.9×10^{15}	1.5×10^{19}
Density (ρ), g cm^{-3}	1.0	1.0
X-ray quantum energy (E), eV	400	400
X-ray intensity (I), W cm^{-2}	$\frac{1}{K}\sqrt{\left(\frac{NEe}{\epsilon\Sigma_e\rho}\right)^3 \frac{F\,\Sigma_a}{\delta^{11}}} = 2.1 \times 10^{11}$	$\frac{1}{K}\sqrt{\left(\frac{NEed}{\epsilon\Sigma_e\rho}\right)^3 \frac{G\,\Sigma_a}{\delta^{14}}} = 3.9 \times 10^{12}$
Pulse length (Δt), seconds	$\frac{\delta^{2/3}}{[F\,I\,K\,\Sigma_a]^{1/3}} = 5.2 \times 10^{-12}$	$\frac{\delta^{5/3}}{d\,[G\,I\,K\,\Sigma_a]^{1/3}} = 2.6 \times 10^{-12}$
Scattering efficiency	10^{-2}	10^{-2}
Exposure, J cm^{-2}	1.1×10^{-2}	10^{-1}

radiation—poorer at longer wavelengths because of diffraction and at shorter wavelengths because of long electron range. Exposures as low as 0.01 joule per square centimeter are sufficient for special photoresist materials (*35, 36*).

To reconstruct a photoresist hologram, one must first make a transmission electron microgram, an enlarged photographic replica, which is subsequently viewed by optical laser illumination to give a further magnified, three-dimensional visible image of the original specimen. Alternatively, a transmission electron microscope can scan the photoresist for analysis by digital computation (*37*).

High-Intensity Holography

In Table 4 the relations presented above are evaluated for two typical hypothetical cases, assuming that coherent radiation at the wavelength of the nitrogen resonance in protein will be available.

The first specimen is an array of protein structures, each having a typical dimension of ~ 100 nm, embedded in a transparent (waterlike) cytoplasm. We wish to study the configurations—that is, to resolve the shapes and surface details of the protein structures—and so specify that $\delta < d$.

The second specimen is a cell membrane, comprising globular protein molecules embedded in a lipid bilayer. For this case, the typical dimension d is smaller than the required resolution δ. We have assumed that the expanding protein molecules will not have begun to overlap before the exposure is completed.

In both cases, the intensity requirements turn out to be quite modest in comparison with the performance of many lasers that operate at longer wavelengths; except for the extremely short pulse duration required to prevent blurring, there is reason to hope that these two snapshots could be made.

Practical Considerations

So far, we have assumed that many challenging technical problems can be solved. Here we note the most serious problems and discuss some conceivable approaches to their solution.

Development of a source that can generate intense coherent radiation at the precise wavelength (or wavelengths?) at which nitrogen in proteins has its maximum scattering cross section will be a major challenge. Perhaps nonlinear mixing with tunable optical radiation will be necessary.

Termination of exposure at the maximum time demanded by Eq. 2 with the corresponding minimum intensity given by Eq. 4 is a major challenge, since it is likely that the laser burst will be longer, and its intensity will probably vary with time. A shutter or gate, somewhere in the system, that operates when full intensity is reached is essential.

In principle, photoelectric recording could be time-gated (*33*). However, complexity, the precision required of the electronics, and the blurring associated with the initial electron velocity distribution (*3*) make this approach unattractive. On the other hand, photoresist recording is not likely to be gatable, so that exposure control must be provided elsewhere in the system; where it is provided depends on the geometry.

"Far-field Fraunhofer" geometry (the limiting case of Fresnel transform holography, when $b\lambda >> d^2$) requires long temporal coherence length and, to preserve the high contrast associated with resonance, a shadow foil that attenuates the reference wave (Fig. 1a). This foil must be homogeneous to within a fraction of a wavelength and must not appreciably degrade spatial coherence. In this inherently simple geometry, no other "optical" element is needed, however.

Leith-Upatnieks holography (*20*) requires a mirror. A synthetic Bragg crystal (*38*) may suffice, and thermal expansion or photoelectron emission can provide automatically time-gated reflection. The mirror can serve as a shadow foil and, with reduced reflectivity, give enhanced contrast.

Concluding Remarks

Our studies have led us to the following conclusions:

1) X-ray sources for microholography of living specimens must be single-shot, high-intensity devices.

2) There is growing confidence that lasers or other sources for this region of the spectrum can be developed with adequate intensity and coherence, and that they can be accessible to experimenters.

3) Maximum contrast between nitrogenous and other constituents of biomatter will be obtained for wavelengths near 3.0 nm, between the absorption edges of oxygen and nitrogen.

4) For holography of the interiors of specimens, this is the optimum wavelength.

5) Strong resonances of nitrogen compounds are probable at this wavelength, further enhancing contrast between nucleic acid or protein and water.

6) The resolutions of most photoresist materials are near their maxima at this wavelength.

7) Microholography offers a unique opportunity for studies of structures and changes of structure accompanying living processes, with nanometer space resolution and picosecond time resolution.

The biological application addressed in this article is, of course, only one of many kinds of problems that may benefit from holography at short wavelengths. However, we believe that it is a particularly promising application for x-ray holography with short-burst, high-intensity sources in the regime in which hydrodynamic expansion, rather than Brownian motion, chemical change, metabolic processes, change of phase, or diffusion, limits the resolution by blurring the holograms.

References and Notes

1. A. Baez, *J. Opt. Soc. Am.* **42**, 756 (1952); ——— and H. El-Sum, *X-Ray Microscopy and Microradiography* (Academic Press, New York, 1957), pp. 347–366.
2. J. Kirz and D. Sayre, in *Synchrotron Radiation Research*, H. Winick and S. Doniach, Eds. (Plenum, New York, 1981), chapter 8.
3. J. Solem, G. Baldwin, G. Chapline, paper O-4, presented at the LASER-81 International Conference, New Orleans, La., 15 December 1981.
4. The findings are reported in more detail in J. C. Solem, *Univ. Calif. Los Alamos Nat. Lab. Rep. LA-9508-MS* (1982).
5. Symbols: a, characteristic transverse dimension of specimen; b, distance from specimen to recording surface; c, speed of light; d, characteristic transverse dimension of opaque structure within specimen; E, photon energy; e, electronic charge; F and G, dimensionless constants related to equation of state and heat transport; h, Planck's constant; I, x-ray intensity; K, number of protein or nucleic acid units per gram of specimen; x, x-ray temporal coherence length; δ, linear resolution, referred to specimen; Δ, linear resolution, referred to recording medium (for instance, grain size); Δt, optimum exposure time; ϵ, quantum efficiency of recording medium; λ, x-ray wavelength; μ, $\sqrt{1 - (\lambda/\delta)^2}$; ξ, minimum useful signal-to-noise ratio of the hologram; ρ, density; Σ, total cross section of a protein or nucleic acid unit; Σ_e, elastic cross section of a protein or nucleic acid unit, and Σ_a, absorption cross section of a protein or nucleic acid unit.
6. L. Mandel and E. Wolf, *Rev. Mod. Phys.* **37**, 232 (1965).
7. LASER-81 International Conference, New Orleans, La., sessions H and O, 15 December 1981; American Physical Society spring meeting, Washington, D.C., session AC, 20 April 1982 [abstracts appear in *Bull. Am. Phys. Soc.* **27**, 452 (1982)].
8. H. Egger, H. Pummer, C. Rhodes, *Laser Focus* **18** (No. 6), 59 (1982).
9. J. Spencer and H. Winick, in *Synchrotron Radiation Research*, H. Winick and S. Doniach, Eds. (Plenum, New York, 1981), chapter 21.
10. G. Chapline and R. Carman, paper H-2, presented at the LASER-81 International Conference, New Orleans, La., 15 December 1981.
11. G. Pert, *Phys. Bull.* **33**, 92 (1982).
12. G. Baldwin, J. Solem, V. Gol'danskii, *Rev. Mod. Phys.* **53**, 644 (1981).
13. P. Jaeglé, paper H-4, presented at the LASER-81 International Conference, New Orleans, La., 15 December 1981; G. Pert (*11*). There are also unconfirmed reports [*Aviation Week*, 23 February 1981; *Laser Focus*, April 1981; A. L. Robinson, *Science* **215**, 488 (1982)] that 1.4-nm laser operation has been successfully accomplished.
14. D. Gabor, *Nature (London)* **161**, 777 (1948).
15. ———, *Proc. R. Soc. London Ser. A* **197**, 454 (1949).
16. G. Stroke, *An Introduction to Coherent Optics*

and Holography (Academic Press, New York, 1969).
17. The temporal coherence requirements given in Table 1 were obtained by an elementary geometric argument involving partially overlapping wave trains. The reference beam's intensity was assumed to be spatially graded with a shadow foil to maximize the fringe contrast.
18. G. Stroke, *Optique des Rayons X et Microanalyse* (Hermann, Paris, 1966), p. 43.
19. J. De Velis, G. Parrent, Jr., B. Thompson, *J. Opt. Soc. Am.* **56**, 423 (1966).
20. E. Leith and J. Upatnieks, *ibid.* **53**, 1377 (1963).
21. G. Stroke and D. Falconer, *ibid.* **55**, 595 (1965); G. Stroke and R. Restrick, *Appl. Phys. Lett.* 7, 229 (1966).
22. G. Rogers and J. Palmer, *J. Microsc.* **89**, 125 (1969).
23. This method has been considered by J. Kare in an unpublished document on x-ray holography.
24. Cross sections are from the ENDF/B Photon Interaction Cross Section Library, Radiation Shielding Information Center, Oak Ridge National Laboratory, tape DLC-7. We appreciate the help of J. H. Hubbell of the National Bureau of Standards in locating this material.
25. Absorption-edge energies are from C. Lederer and V. Shirley, Eds., *Table of Isotopes* (Wiley, New York, ed. 7, 1978).
26. M. Nakamura *et al.*, *Phys. Rev.* **178**, 80 (1969); G. King, F. Read, M. Tronc, *Chem. Phys. Lett.* **52**, 50 (1977).
27. A. Bianconi, H. Petersen, F. Brown, R. Bachrach, *Phys. Rev. A* **17**, 1907 (1978).
28. In complicated molecules, the lowest unfilled molecular orbital will be of very low energy in comparison with *K*-shell binding energy. These resonances will therefore have nearly the same photon energy in all proteins and will have comparable cross sections.
29. H. Frauenfelder and M. C. Marden, in *Physics Vade Mecum*, H. Andersen, Ed. (American Institute of Physics, New York, 1981), section 6.03.
30. Both the absorption and scattering cross sections of a large, completely opaque scatterer approach the geometric cross section [see, for example, J. Jackson, *Classical Electrodynamics* (Wiley, New York, 1962), p. 299]. The case of semiopaque scatterers has been analyzed for particle scattering by heavy nuclei [see, for example, S. Wallace, *Ann. Phys.* **78**, 190 (1973)]. The application of eikonal theory to the diffraction holography of protein molecules is discussed by J. Solem and G. Chapline (in preparation).
31. S. Aoki, Y. Ichihara, S. Kikuta, *Jpn. J. Appl. Phys.* **11**, 1857 (1972); S. Aoki and S. Kikuta, *ibid.* **13**, 1385 (1974); B. Reuter and H. Mahr, *J. Phys. E* **9**, 746 (1976).
32. R. Mueller and S. Jorna, *Appl. Opt.* **16**, 525 (1977).
33. G. Bjorklund, *Stanford Microwave Lab. Rep. 2339* (1974).
34. R. Feder, E. Spiller, J. Topalian, A. Broers, W. Gudat, B. Panessa, Z. Zadunaisky, J. Sedat, *Science* **197**, 259 (1977).
35. R. Feder, E. Spiller, J. Topalian, *Polym. Eng. Sci.* **17**, 385 (1977).
36. Fourier transform holography presents a difficult choice. Fine-grain photographic emulsions and photoresists have comparable figures of merit when compared on the basis of sensitivity (J cm^{-2}) and grain size (cm^2). A microchannel plate in combination with a CsI photocathode could have much higher figure of merit and be electronically time-gatable; however, unavailability of large microchannel plates and nonlinearity of gain mitigate against their use at present [B. Henke, J. Knauer, K. Premaratne, *J. Appl. Phys.* **52**, 1509 (1981)].
37. A hologram provides more than a stereoscopic view; it provides quantitative positional information about all structural elements that are visible within a restricted range of angle. Besides the magnified image of the entire specimen obtained by the usual holographic reconstruction, one can obtain planar cross sections for various depths and inclinations, using well-developed computer techniques.
38. B. Henke, *Adv. X-ray Anal.* **7**, 460 (1965); E. Spiller, "Evaporated multilayer dispersion elements," in *Low Energy X-ray Diagnostics* (American Institute of Physics, New York, 1981).
39. A. Kondratenko and A. Skrinsky, *Optical Information Processing* (Plenum, New York, 1977), vol. 2.
40. We wish to acknowledge G. Chapline for his participation and for calling our attention to the nitrogen resonance, J. Kirz for sharing his wisdom in the field of x-ray microscopy, A. Petschek for his helpful criticism, and F. Harlow for the numerical hydrodynamic calculations.

Liquid Chromatography in 1982

David H. Freeman

The liquid chromatograph has become the most powerful instrument for separations available in chemistry. At the center of its capability is an array of new selective sorptive effects which are being harnessed to solve many practical problems. Research in this area is yielding new insights into interactions in liquids. The advances in liquid chromatography are too numerous to summarize in a short article; instead, an attempt will be made to review some of the more interesting trends.

Liquid chromatography (LC) was first reported in 1906 by Michael Tswett, a Russian botanist. The technique was used to separate plant pigments. Tswett's ideas were expressed with polemic views that made the ideas unattractive to the chemical profession. In the early 1930's the technique was revived, and a growth period of refinement and inventiveness began (*1*). The improvement LC offered over other separation techniques was widely noted in 1971, when the Nobel laureate R. B. Woodward reported a definitive separation of remarkably similar vitamin B_{12} intermediates (*2*), as shown in Fig. 1.

Several years earlier, commercial LC instrumentation had started to become a growth industry. The popularity of the technique since then has grown enormously. Liquid chromatography now dominates the analytical chemistry market and may be a billion-dollar industry by 1985 (*3*). With LC, many chemical separation problems are now being solved, often quickly, by methods that nonspecialists can learn with a little practice. Its success is comparable to that of gas chromatography two decades ago and can be expected to continue.

Liquid chromatography has expanded into a wide range of scientific and industrial applications. It plays a major role in qualitative and quantitative analysis, is a powerful method for group separations, and is used to isolate or analyze products from the mixtures that form during chemical synthesis. It is applied, for example, for quality control of pharmaceuticals, to measure chemicals in foods, to investigate the chemistry and metabolism of biological systems, to aid forensic science, and to help measure unsafe chemicals in the environment. An illustrative application to clinical chemistry is shown in Fig. 2 (*4*).

Established LC separation procedures are available for amino acids, proteins, nucleic acids, lipids, terpenoids, steroids, carbohydrates, drugs, pesticides, petrochemicals, antibiotics, and inorganic and organo-inorganic compounds. The applicability of the technique is rarely limited. Technical and scientific articles on the subject are appearing at the rate of 3000 per year.

Apparatus

An LC separation begins when a small volume of liquid containing a dissolved sample mixture is injected into a moving liquid carrier. The apparatus is shown schematically in Fig. 3. The sample is transported by the carrier stream as it flows through the chromatographic column. This is a cylindrical bed packed with fine sorptive particles, averaging 10 micrometers or less in size. Because the particles resist the flow of liquid, carrier delivery and liquid sample injection must take place at back pressures up to a few hundred atmospheres. Sample injection is usually done with an injection valve, as shown in Fig. 4.

David H. Freeman is a professor in the Department of Chemistry and the Chesapeake Biological Laboratory, University of Maryland, College Park 20742.

0036-8075/82/1015-0235$01.00/0